Modeling of Turbulent Melt Flow and Solidification Processes in Steel Continuous Caster with the Open Source Software Package OpenFOAM

A. Vakhrushev[1], A. Ludwig[1,2], M. Wu[2], Y. Tang[3], G. Nitzl[4], G. Hackl[3]

[1] Christian Doppler Laboratory for Multiphase Modeling of Metallurgical Processes, University of Leoben, A-8700 Leoben, Austria
[2] Simulation and Modeling of Metallurgical Processes, Department of Metallurgy, University of Leoben, A-8700 Leoben, Austria
[3] RHI AG, Technology Center, Standort Leoben, Magnesitstrasse 2, A-8700 Leoben, Austria
[4] RHI AG, 1100 Vienna, Wienerberstrasse 11, Austria

Abstract

Advanced implementation of solidification modeling using open source CFD software, which is of the great importance for the steel industry and relevant application fields, is introduced. Simulation results of the solidification process in the continuous caster are presented, under consideration of the presence of a highly turbulent flow. A mixture solidification model is employed in order to study the interaction between the melt flow and the growing two-phase region. Additionally, a porous resistance formulation for the Darcy law is used to track the flow evolution inside the solidifying mushy zone. The open source software package OpenFOAM is used as the main simulation tool. New solvers for calculating transient turbulent flow and heat transfer along with solidification were developed using the object-oriented concept of the OpenFOAM package. Case files for the solidification model are ordered according to the designed structure of the control dictionaries with a flexible input format. The implementation of additional libraries required boundary conditions, and "temperature-solid fraction" curves were created. The reliability of different RANS turbulent models for the solidification modeling is studied.

Keywords

Numerical modeling, solidification, multiphase flow, turbulence, open source, OpenFOAM

1. INTRODUCTION

The numerical simulation of various physical processes is a key issue in the modern CFD research field. In certain specific cases, it is the unique tool that enables the investigated phenomena to be examined in detail. Solidification in the continuous casting devices is the instance of the corresponding complex process, combining the highly turbulent flow, which interacts with the two phase region called the mushy zone. All considered processes are followed by the phase transition, latent heat diffusion / absorption due to the phase change, etc. Industrial measurements in continuous casting can only produce information regarding the total mass flow rate of the liquid melt, casting speed, surface heat flux extraction values, slag interface oscillations and similar available qualities. However, it is almost impossible to read process parameters from inside the mold due to the high temperatures and ferrostatic pressure during casting. On the one hand, physical experiments with water modeling facilitate an understanding of the hydrodynamics of the turbulent flow in the continuous caster. On the other hand, the phase transition and the influence of the mushy zone presence are not taken into account. Thereby, the numerical simulation using the CFD approach plays a rather important role in continuous casting modeling.

A wide range of commercial software is presented in the CFD market. However, some types are confined to solving a specific problem, others provide a relatively general solution. The common disadvantage of most commercial CFD software is the inaccessibility of the numerical model internals being used. Thus, it is comparatively difficult to debug the numerical solution or modify and improve the numerical model. Nowadays, open source code CFD software is intensively developed, providing a real alternative to the commercial implementations. The OpenFOAM package represents a remarkable simulation toolkit for the CFD field based on the Finite Volume Method (FVM) for the arbitrary polyhedral meshes for single and multiphase flows. It can also be extended to include various additional numerical methods that are not the topic here. The current work focuses on solidification modeling with an application for continuous casting using OpenFOAM as the main programming tool.

A number of the developed numerical models to account for both fluid flow and heat transfer, incorporating the kinetics of the solidification [1-2] are know from the literature. Unfortunately, only the laminar behavior of the solidified liquid melt is included in most of the recent solidification models [3-6]. In the presented studies, the turbulence model considering multiphase media as a viscous mixture is used to simulate solidification in the steel continuous caster. The approaches for handling the turbulence during solidification reported in contributions [7-10] are used. Porous resistance of the two-phase region is combined with the heat transfer modeling, taking into account the influence of the turbulent flow [11-12]. The presented work includes the numerical model description along with the comparison between OpenFOAM and FLUENT results for the 2D benchmark [12]. Finally, a numerical simulation is performed for the real 3D geometry of the steel continuous caster. The quantitative and qualitative verification of the numerical solution with the OpenFOAM solver is carried out based on the experimental measurements and simulation results, obtained by means of the FLUENT software.

2. NUMERICAL MODEL

In presented study, the solidification process is considered along with a highly turbulent flow. There are a number of approaches for modeling solidification that are widely used in the modern CFD field [13]. Some of these use a fixed numerical grid and averaged physical properties of the solidified fluid, others consider front tracking between solid and liquid phases along with adaptive mesh refinement, etc. For the study currently presented, a fixed finite volume mesh is used with a so-called collocated or non-staggered variable arrangement (Rhie and Chow [14], Peri□[15]), where all physical values share the same control volumes (CV), and all flux variables reside on the CV faces. The generalized form of the divergence theorem is used throughout the discretization procedure to represent mass, momentum and energy conservation laws in integral form over the control volume. Unsteady formulation is used to track time-dependent effects during solidification.

Additional assumptions are used to model the investigated phenomena: the multiphase system is described as a viscous fluid with a mixture of properties [3-6], thus it is assumed that the integration control volume is large enough to incorporate a representative amount of the liquid and solid phase in order to mimic the mushy zone; the mixture continuum combines liquid l-phase and solid s-phase (quantified by the corresponding volume fractions f_l and f_s), which changes continuously from a pure liquid region, through the mushy zone (two phase region), to the complete solid region; the solidified shell along the mold walls morphologically represents the columnar phase (dendrites), which is moving with a constant

pulling (casting) velocity $\vec{u}_s$. The amount of the solid phase is predefined with a solid fraction / temperature curve varying for different materials, which is described later.

The Navier-Stokes equations with an assumption of the liquid incompressibility are used to simulate the melt motion. Only one set of equations is formulated for both phases in the Eulerian frame of the reference. The mixture velocity $\vec{u} = f_l \vec{u}_l + f_s \vec{u}_s$ represents a weighted sum of the liquid and solid velocities with the phase fractions as weighting factors. Thereby, the equation system consisting of the continuity and momentum equations is

$$\nabla \cdot \vec{u} = 0, \tag{1}$$

$$\rho \frac{\partial \vec{u}}{\partial t} + \rho \nabla \cdot (\vec{u} \otimes \vec{u}) = -\nabla p + \nabla(\mu_{\text{eff}} \nabla \cdot \vec{u}) + \rho \vec{g} + \vec{S}_{\text{mon}}. \tag{2}$$

It should be noted that the effective dynamic viscosity of the liquid μ_{eff} in the momentum equation (2) is variable throughout the calculation domain due to the turbulence effects. The multiphase behavior of the mixture is defined by the source tem $\vec{S}_{\text{mon}}$ in the same equation, which represents drag force inside the porous region, formed by dendrites. It is modeled based on the Blake-Kozeny law:

$$\vec{S}_{\text{mon}} = -\frac{\mu_l}{K} \cdot (\vec{u} - \vec{u}_s), \tag{3}$$

where μ_l represents laminar viscosity and $(\vec{u} - \vec{u}_s)$ is a relative velocity of the mixture in the porous region. The permeability K of the mushy zone depends on the quantity of the solid phase and the characteristic size of the dendrites, referred to by Gu and Beckermann as the primary arm spacing λ_1 [16]:

$$K = \frac{(1 - f_s)^3}{f_s^2} \cdot 6 \cdot 10^{-4} \cdot \lambda_1^2. \tag{4}$$

To track the evolution of the solid phase, the prescribed relation between solid fraction, f_s and temperature T of different types (e.g. lever rule, Gulliver-Scheil) is used.

The complexity of the numerical modeling of the solidification processes the continuous casting arises mostly due to the transition from the completely turbulent flow to the motion of the solid body with the prescribed constant velocity. Thus, it is desirable to employ a comprehensive model, which incorporates turbulent core description along with a laminar sublayer and a "solid body" behavior for the limit case $f_s = 1$. In the presented study, a RANS turbulence model is used, based on a low Reynolds number k-ε model, introduced by Prescott and Incropera [7-10]:

$$\frac{\partial(\rho k)}{\partial t} + \nabla \cdot (\rho \vec{u} k) = \nabla \cdot \left(\left(\mu_l + \frac{\mu_t}{\text{Pr}_{t,k}} \right) \nabla k \right) + G - \rho \varepsilon + S_k, \tag{5}$$

$$\frac{\partial(\rho \varepsilon)}{\partial t} + \nabla \cdot (\rho \vec{u} \varepsilon) = \nabla \cdot \left(\left(\mu_l + \frac{\mu_t}{\text{Pr}_{t,\varepsilon}} \right) \nabla \varepsilon \right) + C_1 G \frac{\varepsilon}{k} - C_2 \rho \frac{\varepsilon^2}{k} + S_\varepsilon, \tag{6}$$

$$S_k = -\frac{\mu_l}{K} \cdot k, \quad S_\varepsilon = -\frac{\mu_l}{K} \cdot \varepsilon, \tag{7}$$

where $Pr_{t,k}$=1.0, and $Pr_{t,}$=1.3 are the turbulent Prandtl numbers for k and respectively; G is the shear production of turbulence kinetic energy [7-10].

Equations (5-7) allow the turbulence during solidification to be handled, where turbulence parameters k and are dumped within porous region according to the formulation (7). The permeability of a coherent mushy zone is decreasing based on the relation (4) along with a growing solid fraction value.

For the closure of the solidification model system, it is necessary to introduce the energy equation:

$$\frac{\partial h}{\partial t} + \nabla \cdot (\vec{u} h) = \nabla \cdot \Gamma_{\text{eff}} \nabla T + S_e . \tag{8}$$

Equation (8) is applied to the entire domain, where h is the sensitive enthalpy $h = h_{\text{ref}} + \int_{T_{\text{ref}}}^{T} c_p dT$. In the presented study, it is assumed that reference enthalpy h_{ref} and temperature T_{ref} are equal to zero, and the specific heat c_p is constant. Thus, sensitive enthalpy can also be rewritten in the form $h = c_p T$.

It is known that a heat of fusion, also called latent heat, is released due to solidification or absorbed during melting for the phase transition from liquid to solid state or vice versa. The latent heat L is taken into account in the model by the use of an additional source term S_e in the energy equation, which represents a combination of the heat release caused by phase change in the course of time and due to the amount advected with a melt

$$S_e = \rho L \partial f_s / \partial t + \rho L \vec{u}_s \cdot \nabla f_s . \tag{9}$$

From the formulation (2) of the momentum conservation and energy transports (8), the influence of turbulence is considered by the effective viscosity $\mu_{\text{eff}} = \mu_l + \mu_t$ and the effective thermal conductivity $\Gamma_{\text{eff}} = \Gamma + \Gamma_t$. Turbulence values are calculated based on model parameters and coefficients: $\mu_t = \rho C_\mu k^2 / \varepsilon$, $\Gamma_t = \mu_t c_p / \text{Pr}_{t,h}$, $C_\mu = 0{,}09$ is a model parameter, $\text{Pr}_{t,h} = 0{,}85$ is the turbulent Prandtl number for the energy equation.

3. SOLUTION ALGORITHM

It is relatively clear that the model described poses a great challenge for numerical implementation, especially for complex 3D geometries. It contains a large amount of nonlinearity, and the question of coupling continuity, momentum, energy and the equations of the turbulent parameters transport arises. For the pressure-velocity coupling, a modified version of the PIMPLE algorithm, implemented in OpenFOAM, is used. The PIMPLE algorithm represents a merged version of the widely used SIMPLE and PISO methods for pressure-velocity coupling [17-18] for the large time-step transient calculations. Internal iteration loops are used, with underelaxations being applied either for the model variables or for the matrices of the linear equations to be solved. The iteration process stabilizes the numerical solution and enable the use of the time-step values, resulting in the Courant number $Co >> 1$.

Other sources of nonlinearity emerge due to the relationship between the permeability of the mushy zone K and the solid fraction f_s. Moreover, according to the formulations (2)-(4) and the energy equation (8), the solidification is strongly coupled with the melt motion due to

convention / diffusion mechanisms of the heat transfer and latent heat release during the phase change. Here, a so-called temperature recovery method is used to couple fluid flow with the heat transfer and solidification [13].

A flow chart of the solidification solver is presented as a generalization of the described algorithm (Fig. 1). It should be noted that all internal loops of the solution algorithm are executed until either the global convergence criterion is fulfilled (for a fully transient solution) or the prescribed number of steps is executed (if a steady state is the aim).

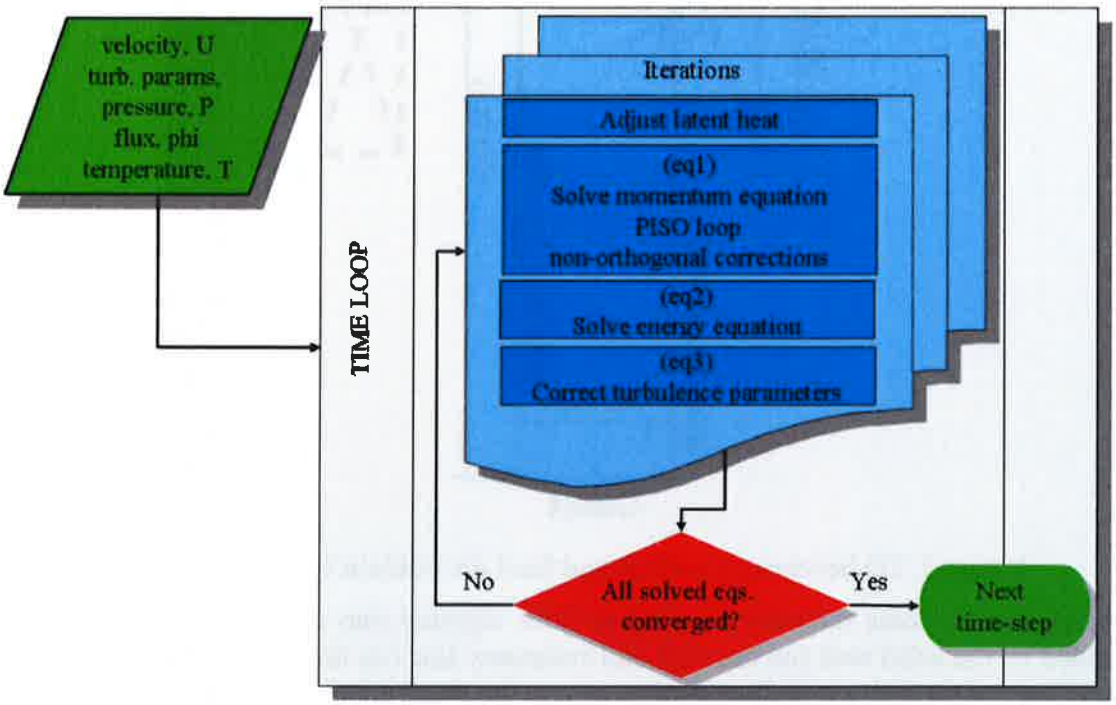

Figure 1. Flow chart of the solidification solver

Additionally, for the more correct numerical treatment, the porous media resistance is included either implicitly in the tensorial resistance or as an explicit source term in the momentum equation. A more detailed description is presented later (e.g. Fig. 6).

In terms of the programming implementation of the described model, the entire advantage of the object-oriented concept of OpenFOAM is used [19]. Developed solvers are provided with the control dictionaries of an arbitrary structure. Thereby, it is possible for users to introduce different solidification model parameters, using designed boundary condition (BC) types for the heat extraction during casting with variable heat flux profiles, etc.

4. SIMULATION RESULTS FOR 2D BENCHMARK

Previous studies are used to verify the implementation of the solidification model using OpenFOAM Finite Volume Method libraries [11-12, 20-21]. First of all, the designed solidification model results for the 2D case were compared with the benchmark, carried out with the FLUENT software. The detailed setup for the reference case is presented [12]. For the purpose of clarification, the calculation domain scheme and the final steady state solution obtained by FLUENT during the discussed benchmark are shown in Fig. 2. Velocity vectors are displayed to indicate the flow direction.

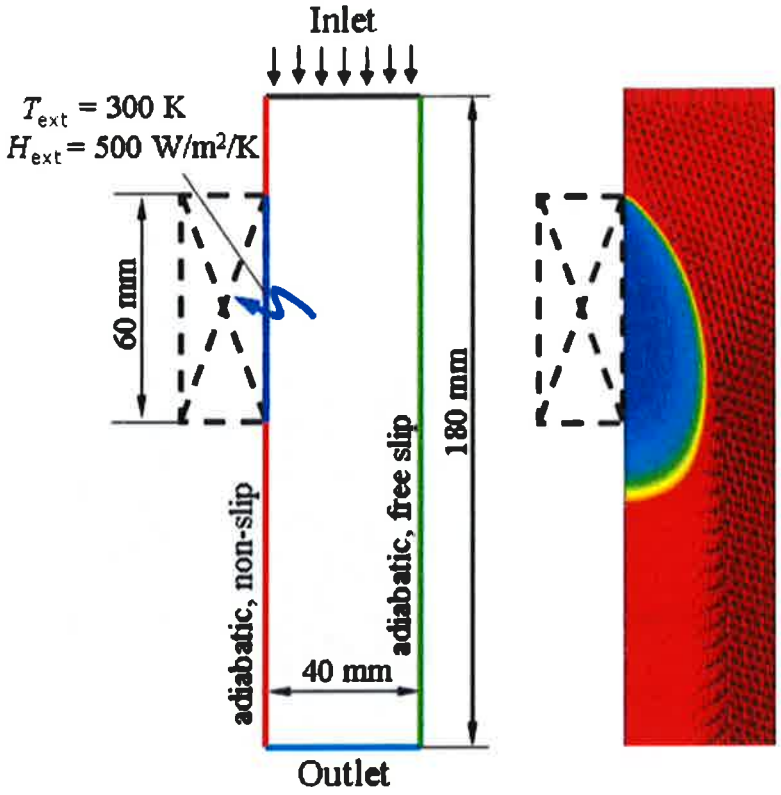

Figure 2. 2D benchmark outline and final distribution of the liquid fraction

In brief, this test case includes a turbulent flow, injected into rectangular domain, which is bounded by the solid wall (on the left) and symmetry line (on the right). The wall is adiabatic overall except for a short cooling section, where the dendritic mushy zone starts growing due to the heat exchange between the liquid melt and the chill. The two-phase zone is assumed to be stationary due to the non-slip boundary condition on the wall.

For the numerical implementation of the solidification model, an additional boundary condition type was programmed in OpenFOAM as the dynamic library. It represents convective heat transfer BC, which is relatively important, since it has a wide application field for simulating heat transfer based on the given value of the Heat Transfer Coefficient (HTC). According to the FLUENT User Guide [22], convective heat transfer BC (excluding radiative heat flux) can be written as follows

$$q = H_f(T_w - T_f) = H_{ext}(T_{ext} - T_w), \tag{9}$$

where q is a heat flux through the boundary; T_f is a fluid temperature right next to the boundary fluid point; T_w represents wall temperature; T_{ext} is external heat-sink temperature (e.g. ambient temperature); H_f and H_{ext} are local fluid and external heat transfer coefficients respectively.

Boundary condition (9) is in fact the heat flux balance equation at the boundary, meaning that no heat should accumulate at the fluid-wall interface. Thereby, it can be reformulated according to the Fourier's law:

$$q_{wall} \equiv H_{ext}(T_{ext} - T_w) \equiv \lambda_f \left(\frac{dT}{dn}\right)_{wall}, \tag{10}$$

where $\vec{n}$ resulting in implicit BC relative to the wall temperature T_w

$$(T_{ext} - T_w) - \frac{L_f}{H_{ext}} \left(\frac{dT}{d\vec{n}} \right)_{wall} = 0. \qquad (11)$$

Thee ordinary differential equation (ODE) for the variable T_w (11) can be solved using any of known numerical approaches for solving ODE.

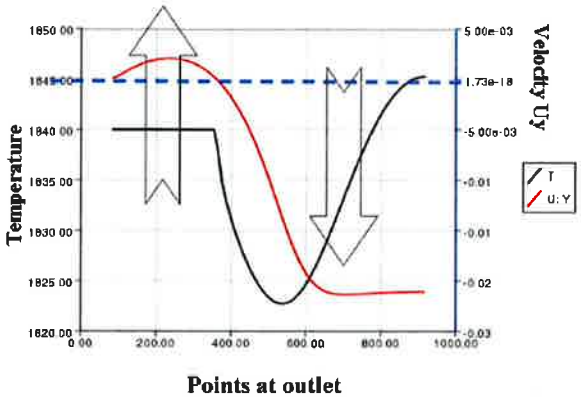

Figure 3. Outlet temperature values dependent on velocity direction

An additional boundary condition is applied for the outlet of the numerical domain. It is dependent on velocity direction (Fig. 3) and is often used in FLUENT simulations. A boundary condition base on the velocity direction can be used to stabilize the solution (e.g. defining laminar backflow). In the presented 2D benchmark, it is utilized in order to set the backflow temperature. To apply this kind of boundary condition in OpenFOAM, the *inletOutlet* type of geometry patch is used.

After the numerical solution was converged to the steady state, a comparison was made based on FLUENT results (Fig. 4-5). Temperature, solid / liquid fraction, velocity field distribution were compared throughout the calculation domain. It should be noted that the same boundary and initial conditions along with the 2nd order of the FV discretization were used both in OpenFOAM and FLUENT solvers' setup. However, a slight difference is still observed in temperature distribution (Fig. 4-a), velocity magnitudes (Fig. 4-b) and liquid fraction values (Fig. 4-c) if compared with results obtained by different software. All plots are presented for the line in the central section across the simulation domain. During numerical studies it was also detected that in many cases boundary values calculated for the Neumann boundary condition type vary in OpenFOAM and FLUENT. However, the inconsistency between two numerical solutions is not significant, therefore it can be stated that the solidification model, implemented as an additional OpenFOAM solver, is verified according to the previous studies based on literature and industrial data.

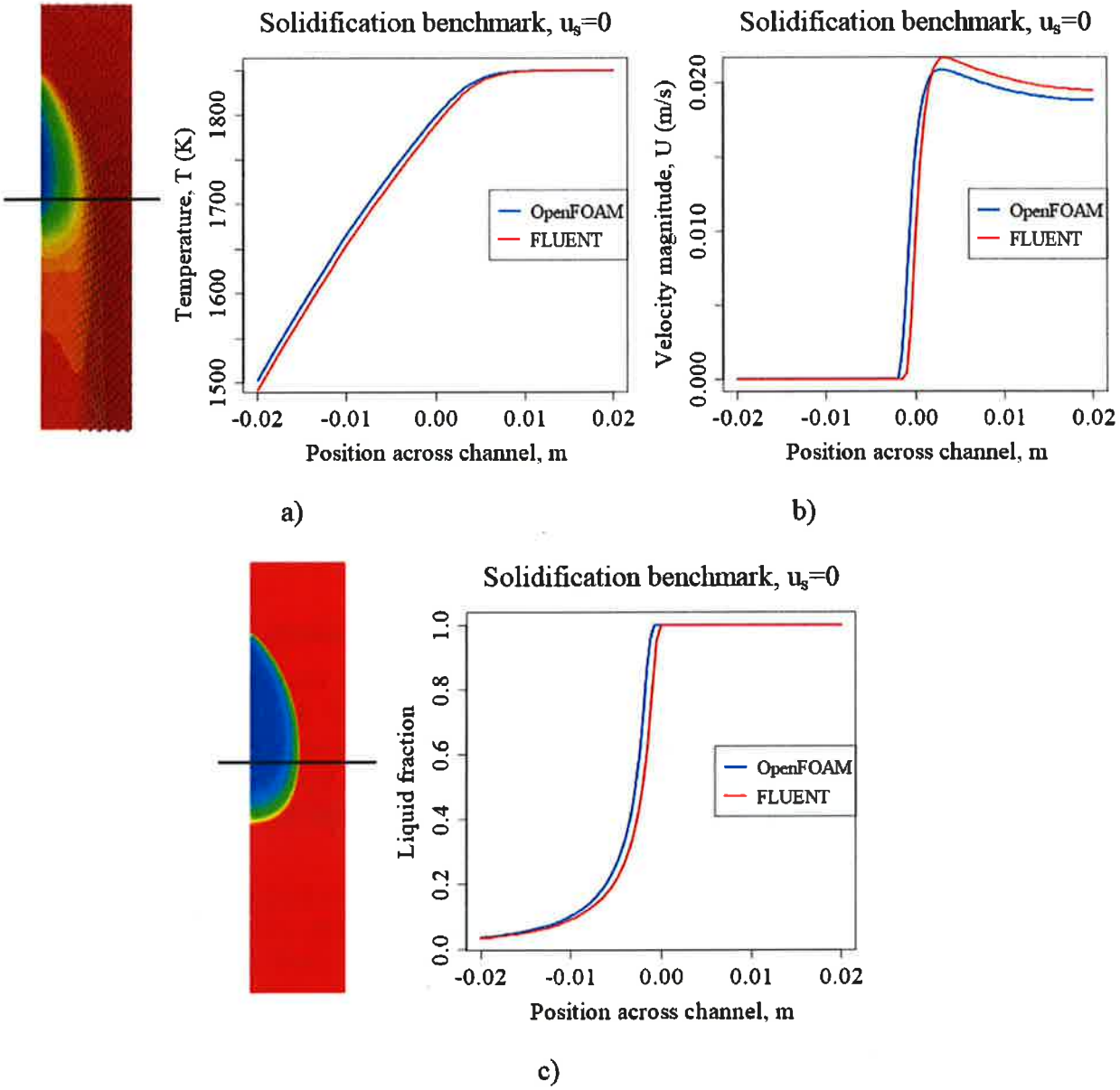

Figure 4. Steady state solution comparison (2D solidification benchmark):
a) temperature field; b) velocity magnitude; c) liquid fraction distribution

The convergence of the numerical solution is of great importance for numerical simulation. Due to the coupling complexity and nonlinearity problems within the considered model, it is clear that the solution converges and meets the predefined assumptions of the model. One of the criteria that can be used for the solution control is the correspondence of the numerical solution to the temperature / solid fraction curve. All internal loops of the calculation algorithm and underelaxations that are applied should lead to the flow chart point, where the phase fraction meets the temperature distribution in each cell of the finite volume mesh with a given accuracy. The results of the test for the given 2D benchmark are shown in Fig. 5. Both solutions converged to the proper $f_s - T$ curve.

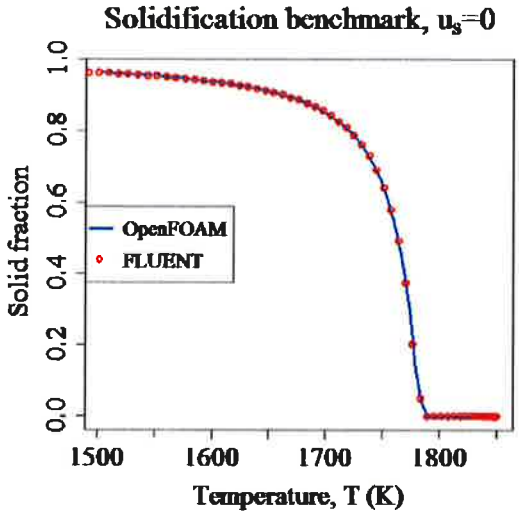

Figure 5. Recovered $f_s - T$ curve based on the calculated temperature and solid fraction field distribution

The influence of the implicit versus explicit formulation of the pressure resistance of the porous mushy zone was investigated for the 2D case (Fig. 6). In both cases, a steady state solution was the aim. For the explicit treatment of the porous resistance (Fig. 6-a), the drag force within the mushy zone was considered as an explicit source term in the momentum equation (2). For the implicit one, a tensorial resistance was used.

From the residual plots in Fig. 6-a, one can see that in the case of explicit porous resistance, the Poisson's equation for pressure will never converge to the given tolerance value due to various fluctuations of the numerical solution. On the contrary, with the tensorial resistance being applied, the total equation system converges very fast (Fig. 6-b), showing the theoretical and practical advantages of the described numerical approach.

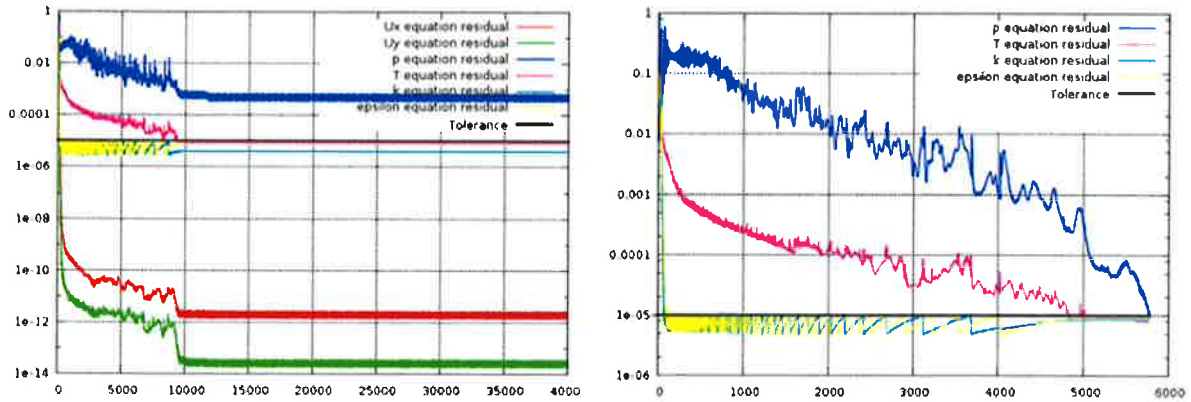

a) b)

Figure 6. Residuals behavior of the numerical solution (2D case):
a) explicit treatment of the porous resistance;
b) explicit tensorial resistance form

5. SIMULATION RESULTS OF 3D CONTINUOUS CASTER

Using the previously described model, the simulation of real continuous caster (CC) was carried out. The simulated geometry of the steel continuous caster with the three-port Submerged Entry Nozzle (SEN) is shown in Fig. 7.

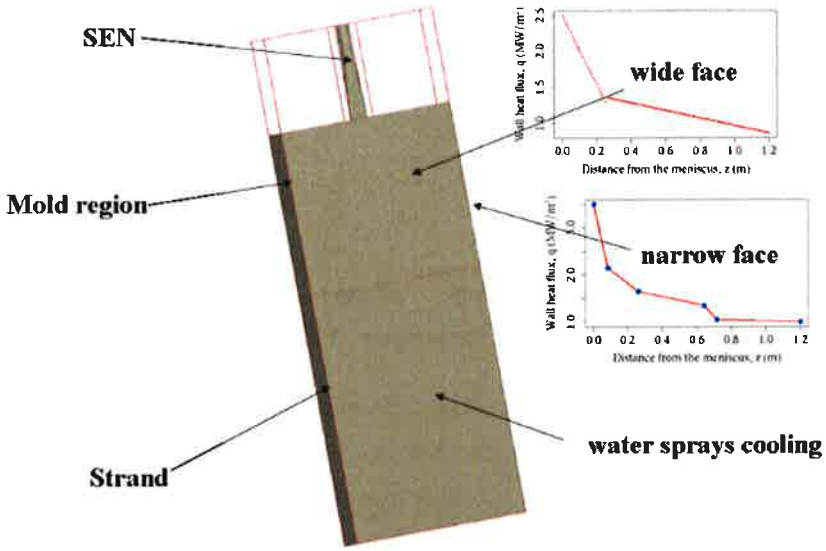

Figure 7. Steel continuous caster geometry with 3-port design SEN; primary and secondary cooling zones are considered

The design of the simulated CC includes the mold part with a liquid melt being injected through the SEN. At the top of the mold, a slag interface is simulated. The primary cooling zone is specified by setting extracted heat flux profiles, which can be measured during industrial processes and provided as external data for the application. The programmed heat flux boundary condition library can accept a general format of the user data (e.g. hyperbolic, polynomial interpolation, piecewise-linear profile, etc.). In order to apply heat flux BC, it is necessary to consider the heat balance at the wall-liquid interface:

$$q_{wall} \equiv \lambda_f \left(\frac{dT}{dn} \right)_{wall} . \qquad (12)$$

The equation (12) for the predefined heat flux as well as the convective heat transfer condition (11) can vary depending on either the laminar or wall function approach being used to calculate wall temperature values [22].

Bilinear interpolation can be used in the numerical grid to reconstruct indeterminate heat flux values. The considered option is relatively useful when several measured points are presented along the whole mold area, but there is a lack of intermediate data. For the presented study, the uniform distributed heat flux profiles are used separately for both wide and narrow faces of the mold depending on the distance from the meniscus (Fig. 7).

The secondary cooling zone presents the strand part being cooled down, for example with water sprays (Fig. 7). From this point onwards, the convective heat transfer is included in the numerical model based on equation (11).

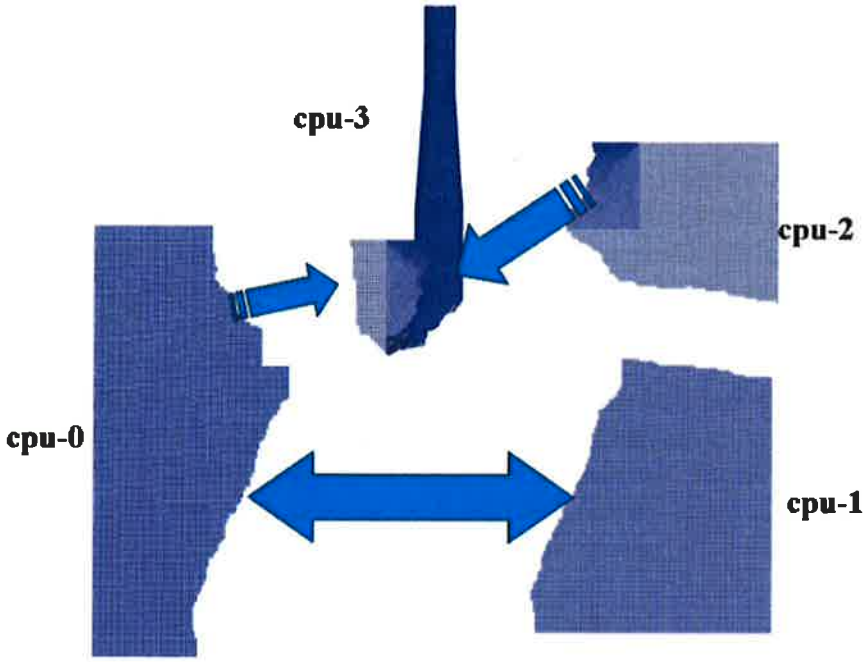

Figure 8. Domain decomposition for the parallel calculations (*metis* method, 4 CPUs)

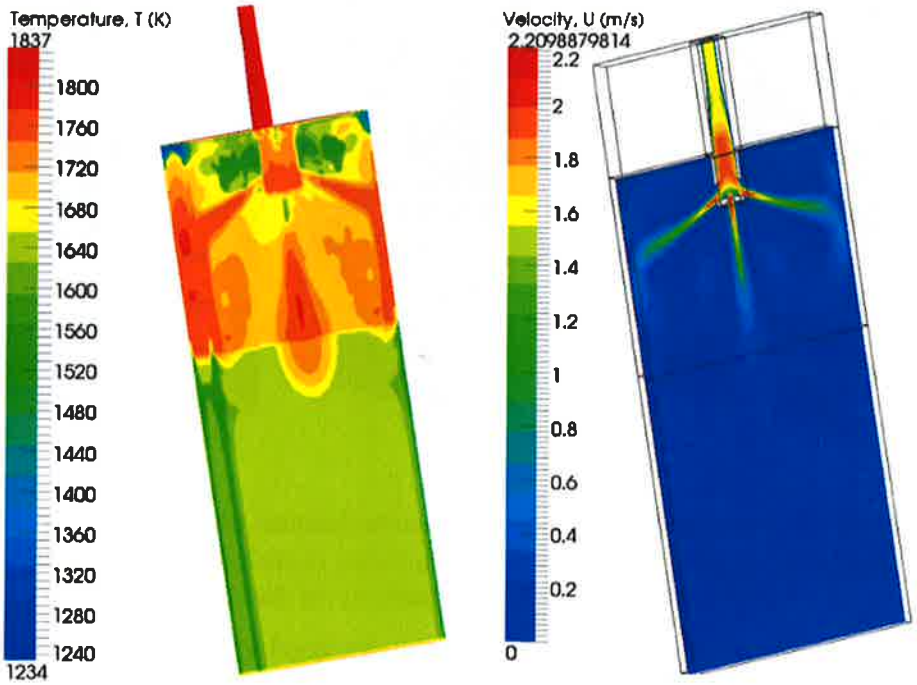

a) b)

Figure 9. Results of the simulation (steady state):
a) temperature distribution on the mold and strand face;
b) velocity magnitude distribution (central plane cross-section)

To improve the performance of the 3D continuous caster simulations, the advantage of the parallel calculations efficiency was used. OpenFOAM demonstrates comparatively good scalability of the parallel execution on the calculation clusters and provides a wide range of decomposition methods. The decomposition method called "*metis*" is appropriate for the complex 3D geometries of the same kind as presented CC. It splits the calculation grid into

the desired number of subdomains, while balancing the number of the finite volume cells presented in each part and minimizing the boundaries between processors. The decomposition of the steel CC geometry for the parallel run using 4 CPUs is schematically represented in Fig. 8.

The previous studies enabled the steady state solution for the considered geometry to be found [11]. Availability of the steady state solution for the 3D case is very rare, and the attempt to obtain it provides an excellent opportunity to carry out additional studies. The results of the numerical simulation are presented in Fig. 9-11. Here one can observe temperature distribution along the mold and strand parts with occurrence of the hot spots at the impeachment points (Fig. 9-a). It is possible to investigate flow pattern (Fig. 9-b) along with turbulence parameter distribution (Fig. 10). An analysis of the numerical solution shows that the generation of most of the turbulence in the simulated case is due to liquid melt jets coming out of the SEN ports and because of the flow-wall interaction (Fig. 10-a). The significant influence of the turbulence on the solidification according to the [12] is predefined by the increase of the effective thermal conductivity near the walls (see Fig. 10-c).

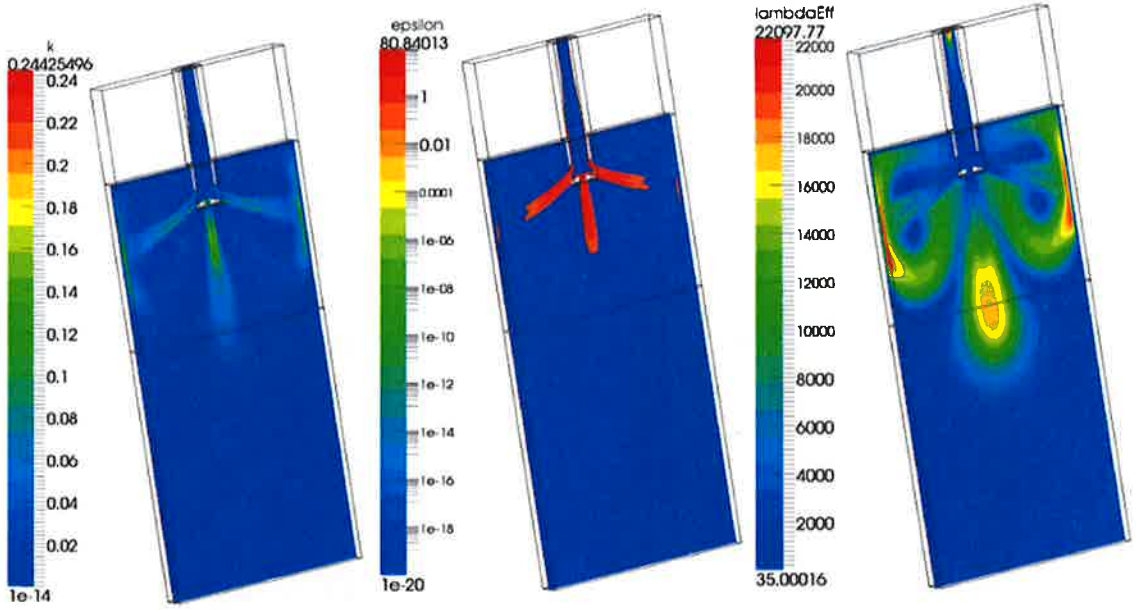

a) b) c)

Figure 10. Turbulent parameter distribution (central plane cross-section):
a) turbulent kinetic energy; b) dissipation rate of turbulent kinetic energy;
c) effective thermal conductivity of the mixture

The steady state solution obtained by means of the designed OpenFOAM solver is compared to the simulation results in FLUENT [11] and the experimental measurements [23].

The characteristic value used to verify the results is the thickness of the so-called solid shell, which corresponds to the solid phase fraction of 80-90%. It is possible to observe the 3D representation of the simulated solid shell in the steel continuous caster (Fig. 11-a), as well as the results of a comparison between previous studies and the experimental data (Fig. 11-b top) and numerical solutions in CFD software of both FLUENT and OpenFOAM. (Fig. 11-b bottom).

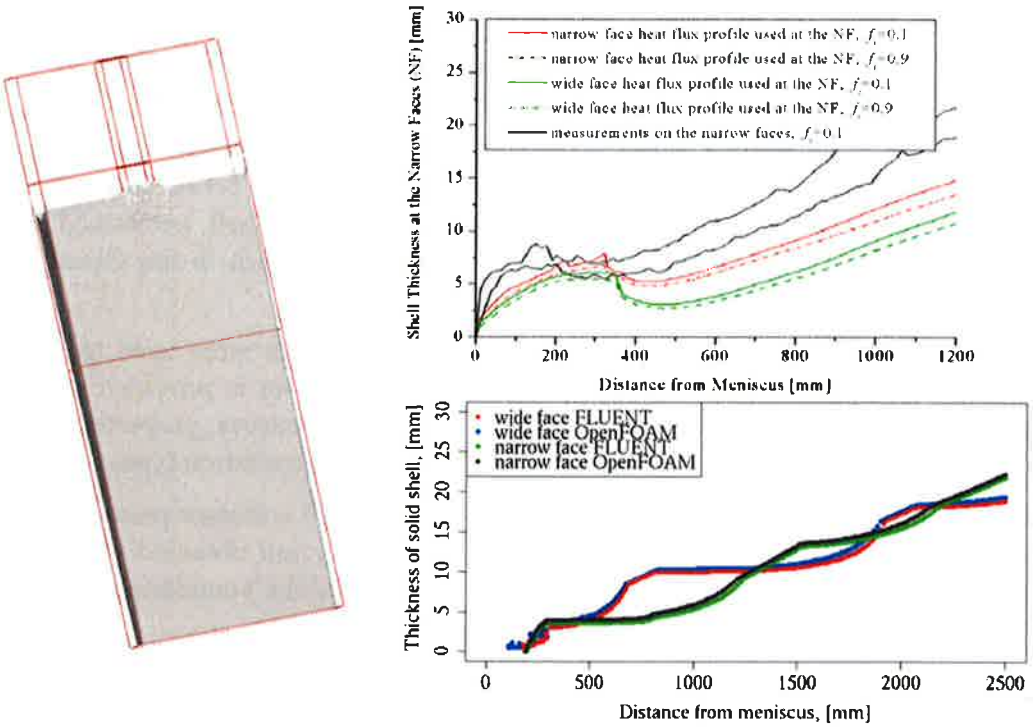

a) b)

Figure 11. Results of the solid shell formation modeling:
a) solid shell surface represented in 3D (f_s = 0,8);
b) comparison of the simulated solid shell thickness
with experimental data [14]

On the one hand, a quantitative comparison of the numerical solution showed slight a difference from the experiment; however, the reason for this is concealed in the different process conditions under which the data was obtained, as explained in [11]. On the other hand, a qualitative comparison showed good agreement between values predicted by the simulation and those measured.

It was also observed that both FLUENT and the developed OpenFOAM solver for solidification modeling produced quite similar results (Fig. 11-b bottom). Thereby, these two CFD software packages can be used as a reference for each other.

6. SUMMARY DISCUSSIONS

Solidification modeling is of great importance for a wide range of fundamental and practical application fields. It helps the investigation of core processes for which industrial measurement methods are inadequate, or which are hard to model by means of physical experiments. Moreover, nowadays a plentitude of CFD simulation tools appear suitable for studying multiphase flows while taking into account coupled mass and heat transfer with the phase transformations. Additional advantages are created by the CFD software with open source code, providing the modification, development and improvement of numerical models. In the presented work, the OpenFOAM CFD software package is used as the main simulation tool.

The mixture model was used for the current study. It includes turbulence modeling by means of the RANS approach along with solidification modeling using the so-called temperature recovery method. The modified RANS turbulence models, based on the assumptions of

Prescott and Incropera [9-10], are used to deal with the interaction between the liquid melt flow and the mushy zone. It is assumed that turbulent parameters are dumped within porous region of the growing columnar phase based on its permeability.

The simulation results obtained with the OpenFOAM solver have been verified numerically, based on the previous studies for both the 2D and the 3D case [11-12], and experimentally with the published data regarding measurements of the solidified shell, performed by Thomas [23]. Good quantitative agreement between the numerical solution in the OpenFOAM and FLUENT software was obtained.

The developed solidification model and the OpenFOAM solver were used to simulate the steel continuous casting for the real CC geometry. The end-user is provided with the wide range of available solver settings: liquid fraction / temperature curves, properties of the liquid melt, solidification properties, a number of designed boundary condition types, etc.

In conclusion, it should be emphasized that open source CFD software provides an efficient modeling tools for preprocessing, running simulations, analyzing obtained numerical results and performing parameter studies. It should be used to extend the boundaries of experimental research work in fields such as solidification and multiphase flow.

NOMENCLATURE

c_p	$J \cdot kg^{-1} \cdot K^{-1}$	specific heat
C_1, C_2, C	1	constant of the standard $k-\varepsilon$ model
f_l, f_s	1	volume fraction of liquid and solid phase
$\vec{g}$	$m \cdot s^{-2}$	gravity acceleration
G	$kg \cdot m^{-1} \cdot s^{-3}$	shear production of turbulence kinetic energy
h	$J \cdot kg^{-1}$	enthalpy
h_{ref}	$J \cdot kg^{-1}$	reference enthalpy at temperature T_{ref}
H_{ext}	$W \cdot m^{-2} K^{-1}$	Heat Transfer Coefficients at the wall
k	$m^2 \cdot s^{-2}$	turbulence kinetic energy per unit of mass
K	m^2	permeability
L	$J \cdot kg^{-1}$	latent heat
p	$N \cdot m^{-2}$	pressure
$Pr_{t,h}$	1	Prandtl number for energy equation
$Pr_{t,k}$	1	Prandtl number for turbulence kinetic energy k
$Pr_{t,\varepsilon}$	1	Prandtl number for turbulence dissipation rate ε
q	$W \cdot m^{-2}$	wall heat flux
Re	1	Reynolds number
S_e	$J \cdot m^{-3} \cdot s^{-1}$	source term for energy equation
S_k	$kg \cdot m^{-1} \cdot s^{-3}$	source term for turbulence kinetic energy
$\vec{S}_{mon}$	$kg \cdot m^{-2} \cdot s^{-2}$	source term for momentum equation
t	s	time
T	K	temperature
T_{ext}	K	external heat-sink temperature
T_{ref}	K	reference temperature for h_{ref}
$\vec{u}$	$m \cdot s^{-1}$	velocity of the mixture
$\vec{u}_{inlet}$	$m \cdot s^{-1}$	inlet velocity
$\vec{u}_l$	$m \cdot s^{-1}$	liquid velocity
$\vec{u}_s$	$m \cdot s^{-1}$	solid velocity
Δx	m	mesh size
ε	$m^2 \cdot s^{-3}$	turbulence dissipation rate per unit of mass
λ	$W \, m^{-1} \cdot K^{-1}$	thermal conductivity
λ_{eff}	$W \, m^{-1} \cdot K^{-1}$	effective thermal conductivity due to turbulence
λ_t	$W \, m^{-1} \cdot K^{-1}$	turbulence thermal conductivity
λ_1	m	primary dendrite arm spacing
ρ	$kg \cdot m^{-3}$	density
μ_{eff}	$kg \cdot m^{-1} \cdot s^{-1}$	dynamic effective viscosity due to turbulence
μ_l	$kg \cdot m^{-1} \cdot s^{-1}$	dynamic liquid viscosity
μ_t	$kg \cdot m^{-1} \cdot s^{-1}$	dynamic turbulence viscosity

REFERENCES

1. M. Rappaz, "Modelling of Microstructure Formation in Solidification Processes", *Intern. Mater. Rev.*, vol. 34, Issue 3, pp. 93-123, 1989.
2. C. Beckermann, and R. Viskanta, "Mathematical modeling of transport phenomena during alloy solidification", *Appl. Mech. Rev.*, vol. 46, pp.1-27, 1993.
3. V.R. Voller, and C. Prakash, "A fixed grid numerical modeling methodology for convection – diffusion mushy region phase-change problems", *Int. J. Heat Mass Transfer*, vol. 30, No. 8, pp. 1709-1719, 1987.
4. V.R. Voller, A.D. Brent, and C. Prakash, "The modeling of heat, mass and solute transport in solidification systems", *Int. J. Heat Mass Transfer*, vol. 32, No. 9, pp. 1719-1719, 1989.
5. V.R. Voller, A.D. Brent, and C. Prakash, "Modeling the mushy region in a binary alloy", *Appl. Math. Modeling*, vol. 14, pp. 320-326, 1990.
6. V.R. Voller, and C.R. Swaminathan, "General source-based method for solidification phase change", *Numerical Heat Transfer*, Part B, vol. 19, pp. 175-189, 1991.
7. P.J. Prescott, and F.P. Incropera, "The effect of turbulence on solidification of a binary metal alloy with electromagnetic stirring", in: *Transport Phenomena in Materials Processing and Manufacturing*, ASME HTD, vol. 280, pp. 59-69, 1994.
8. P.J. Prescott, and F.P. Incropera, "Convective transport phenomena and macrosegregation during solidification of a binary metal alloy: I-Numerical predictions", *J. Heat Transfer*, vol. 116, pp. 735-741, 1994.
9. P.J. Prescott, F.P. Incropera, and D.R. Gaskell, "Convective transport phenomena and macrosegregation during solidification of a binary metal alloy: II-Experiments and comparisons with numerical predictions", *Trans. ASME*, vol. 116, pp. 742-749, 1994.
10. P.J. Prescott, and F.P. Incropera, "The effect of turbulence on solidification of a binary metal alloy with electromagnetic stirring", *Trans. ASME*, vol. 117, pp. 716-724, 1995.
11. C. Pfeiler, "Modeling of Turbulent Particle/Gas Dispersion in the Mold Region and Particle Entrapment into the Solid Shell of a Steel Continuous Caster", PhD thesis, Montanuniversität Leoben (2008).
12. M. Wu, A. Vakhrushev, G. Nummer, C. Pfeiler, A. Kharicha and A. Ludwig, "Importance of Melt Flow in Solidifying Mushy Zone", *Open Transport Phenomena J. – Bentham Open*, vol. 2, pp. 16-23, 2010.
13. Dantzig, J. A, and Michel Rappaz. *Solidification*. 1. ed.: EPFL Press, 2009.
14. Rhie, C.M. and Chow, W.L., "A numerical study of the turbulent flow past an isolated airfoil with trailing edge separation", AIAA-82-0998, AIAA/ASME 3rd Joint Thermophysics, Fluids, Plasma and Heat Transfer Conference, St. Louis, Missouri, 1982.
15. Peri⌊ M., "A Finite Volume method for the prediction of three-dimensional fluid flow in complex ducts", PhD thesis, Imperial College, University of London, 1985.
16. J.P. Gu,and C. Beckermann, "Simulation of convection and macrosegregation in a large steel ingot", *Metall. Mater. Trans. A*, vol. 33A, pp.1357-1366, 1999.
17. S. V. Patankar. *Numerical Heat Transfer and Fluid Flow*. Taylor & Francis, USA, 1980.
18. J. H. Ferziger and M. Peric. *Computational Methods for Fluid Dynamics*. Springer, Germany, 2002.
19. Weller, H.G., Tabor,G., Jasak,H. ,Fureby,C., "A tensorial approach to CFD using object orientated techniques", *Computers in Physics*, vol. 12, pp. 620–631, 1998.
20. C. Pfeiler, B.G. Thomas, M. Wu, A. Ludwig, A. Kharicha, "Solidification and particle entrapment during continuous casting steel", *Steel Res. Int.*, vol. 79, pp. 599-607, 2008.

21. M. Wu, A. Ludwig, C. Pfeiler, F. Mayer, "Multiphase flow modelling and its application potentials in steel continuous casting", *J. of Iron & Steel Res. Int.*, vol. 15 Supplement 1, pp. 30-37, 2008.
22. Fluent: *FLUENT 6.3 User's Guide*, Fluent Inc. (2006).
23. B.G. Thomas, R. O'Malley, D. Stone, "Measurement of temperature, solidification, and microstructure in a continuous cast thin slab", Proceedings of McWASP VIII, TMS Publications, pp. 1185-1198, 1998.